

Origins of Asymmetric Phosphazene Organocatalysis: Computations Reveal a Common Mechanism for Nitro- and Phospho-Aldol Additions

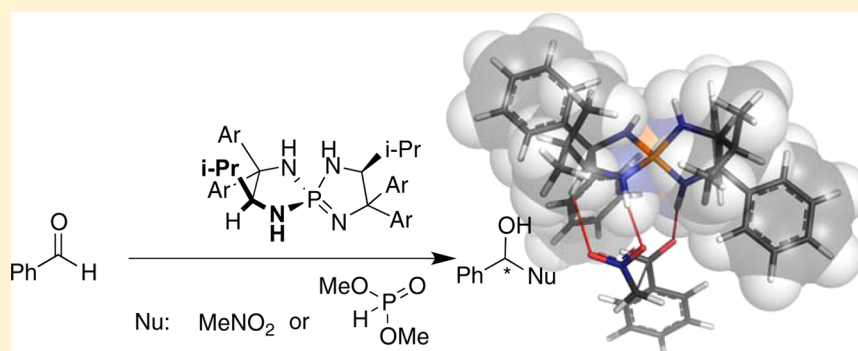
Luis Simón^{*,†} and Robert S. Paton^{*,‡,§}

[†]Facultad de Ciencias Químicas, Universidad de Salamanca, Plaza de los Caídos 1-5, Salamanca E37004, Spain

[‡]Chemistry Research Laboratory, University of Oxford, Mansfield Road, Oxford OX1 3TA, U.K.

[§]Physical and Theoretical Chemistry Laboratory, University of Oxford, South Parks Road, Oxford OX1 3QZ, U.K.

S Supporting Information



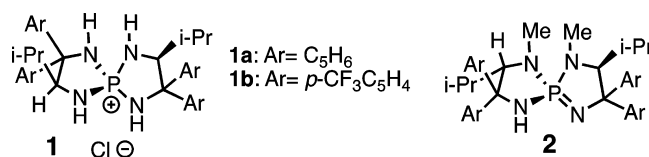
ABSTRACT: We report a hybrid density functional theory–molecular mechanics study of the mechanism of the addition of nitroalkanes and phosphonates to benzaldehyde catalyzed by a chiral phosphazene catalyst developed by Ooi and co-workers. Our results are consistent with a reaction mechanism in which a catalyst molecule simultaneously interacts by hydrogen bonds with the nucleophile and the electrophile, transferring a proton to the aldehyde in concert with carbon–carbon bond formation. Despite the C_2 symmetry of this class of organocatalyst, substrate recognition, and asymmetric induction in both reaction classes studied relies on interactions with nonequivalent N–H bonds that break symmetry. The origin of the stereo and diastereoselectivity is discussed in terms of steric effects and of the conformations adopted by the reactants, and the most favorable transition structure results from minimal geometric distortion energies. A rational model for predicting the major stereoisomer of reactions catalyzed by this chiral phosphazene, based on the qualitative assessment of steric interactions, is given.

INTRODUCTION

In the past decade, organocatalysts containing functional groups able to activate both nucleophilic and electrophilic reactants, typically with H-bonding interactions, have experienced rapid development. These catalysts are able to act simultaneously as proton donors to the electrophile and as proton acceptors from the nucleophile, which acts to minimize the extent of unfavorable charge separation along the reaction coordinate.^{1–10} Phosphoric acids in the BINOP organocatalyst^{11,12} and guanidine,^{13–15} imidodiphosphoric acid,^{16,17} or sulfonic acid⁸ derived organocatalysts exemplify this dual-mode of substrate activation. When employed in asymmetric catalysis, there are relatively few examples of unsymmetrical organocatalysts of this type (such as *N*-triflyl¹⁸ or *N*-phosphinyl¹⁹ BINOL-derived phosphoramides). More commonly, these catalysts display C_2 symmetry, so after the double proton transfer event, the structure of the catalyst is unaltered. By avoiding the formation of a less stable catalyst conformation or tautomer, this phenomenon contributes to a reduction in the activation energy barrier leading to more efficient catalysis.

Recently, many organocatalyst based on phosphonium salts have been described.^{20,21} Within this category, Ooi and co-workers have pioneered the development^{22–33} a set of C_2 -symmetric organocatalysts based on a chiral phosphazene group (Scheme 1), which are readily available from nature's chiral pool as valine. Although in some reactions the catalyst is employed in the form of a pivalate²³ or phenolate²⁸ tetraaminophosphonium salts, more often it is used in its basic phosphazene form, either by

Scheme 1. Structure of Chiral Phosphazene Catalysts 1a, 1b, and 2 Developed by Ooi and Co-Workers^{22–33}



Received: January 9, 2015

Published: February 6, 2015

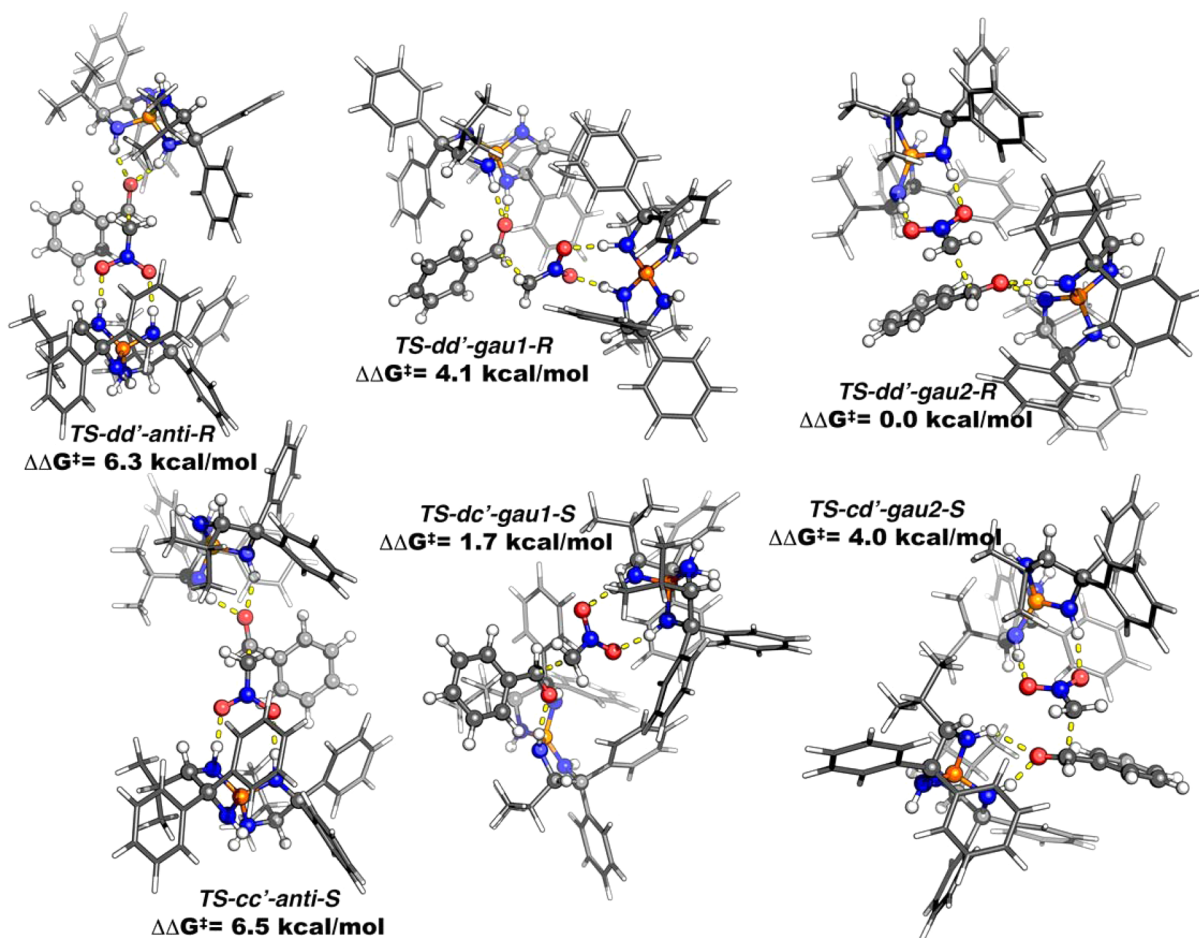


Figure 1. Most stable transition state structures for anti, gauche1, and gauche2 orientations yielding (*R*)- and (*S*)-products. Schematic representation of these structures can be found in the Supporting Information.

the in situ preparation from the reaction of the tetraaminophosphonium chloride of catalyst **1** with potassium *tert*-butoxide^{22,24–26,31} or by the direct employment of catalyst **2**.^{27,29–33} In this case, the phosphacene group basicity is sufficient for the deprotonation of nucleophiles as nitroalkanes or phosphites, as revealed by ¹⁹P NMR spectroscopic studies.^{22,24} The ion pair formed with the protonated organocatalyst, and nitronate or phosphonate anion, is then able to react with an electrophile such as benzaldehyde.

In this paper, we study the mechanism of the asymmetric nucleophilic addition of nitroalkanes and phosphites to aldehydes catalyzed by phosphonium **1**. We consider different mechanisms: the concurrent participation of two catalyst molecules, and the simultaneous proton donor–proton acceptor mechanism involving a single catalyst molecule. We also explain the origin of the enantioselectivity and diastereoselectivity observed in the reactions based on the identification of interactions between the catalyst and the reactants and on the distortion of the catalyst optimal geometry in the TSs.

■ COMPUTATIONAL METHODS

Calculations were performed with Gaussian09.³⁴ The ONIOM^{35–37} QM/MM method, combining the UFF³⁸ molecular mechanics force field for the low level layer with the B3LYP³⁹ density functional and 6-31G(d,p)^{40–42} basis set, was used for the optimization of all stationary points. We favor the employment of a molecular mechanics method to describe the low level layer (over semiempirical methods or quantum chemical calculations with very small basis sets) since the MM force field

by definition includes a description of dispersion effects between all atoms in the MM region and between QM and MM regions. Indeed, this hybrid approach has been shown to be accurate in computational studies of organocatalytic reactions where apolar groups are included in the low level layer.^{2–4,43–46} The partitioning of atoms into the two layers is shown in Figures 1–6 using a “ball-and-stick” representation for the atoms treated by the DFT method and a “wire” representation for the atoms in the low level layer. These figures were prepared using Pymol v0.99.⁴⁷ Single-point energies were evaluated for all optimized structures using the dispersion-corrected ω B97XD⁴⁸ functional with a 6-31++(d,p) basis set. Solvent effects (tetrahydrofuran) were introduced in these calculations by means of an IEFPCM^{49–53} calculation using the SMD intrinsic solvation model.⁵⁴ The Gibbs free-energy correction at 200 K (the temperature employed in experiments) was calculated at the same level of theory used in the optimization, ONIOM(B3LYP/6-31G(d,p):UFF), in which the vibrational entropies were corrected according to the so-called “quasi-harmonic approach”⁵⁵ using a free-rotor approximation for vibrational modes below 100 cm^{–1} and a rigid rotor approximation above this cutoff.⁵⁶ Predictions of enantioselectivity are made on the basis of transition state theory and upon application of the Curtin-Hammett principle: relatively rapid equilibration of prereactive complexes prior to C–C formation dictates that the relative free energies of competing transition states are compared.

The noncovalent interaction (NCI) index was calculated with NCIPLOT^{57,58} from the wB97XD/6-31++(d,p) electron density. Hyperconjugation effects were studied by means of second-order perturbation analysis of the Fock Matrix in the NBO basis performed with NBO v. 3⁵⁹ implemented in Gaussian09, using the wB97XD/6-31++(d,p) wave function.

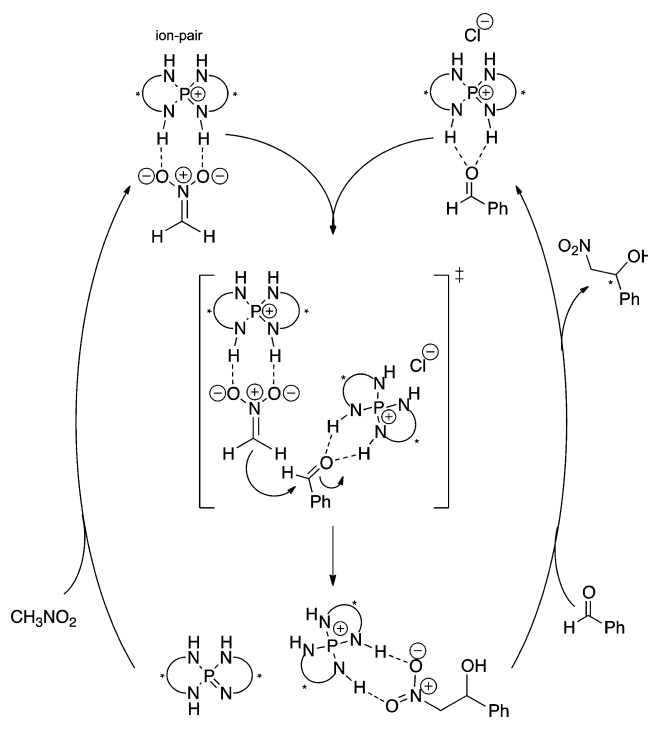
RESULTS AND DISCUSSION

Henry Reaction of Nitromethane and Benzaldehyde Catalyzed by Two 1a Catalyst Molecules. We started our study with the Henry reaction of nitromethane and benzaldehyde catalyzed by 1a.²² Himo and co-workers have found that the rate-determining step in the Henry reaction catalyzed by a tertiary amine from a Cinchona-derived thiourea corresponds to the deprotonation step.⁶⁰ In a related reaction, Dixon and co-workers⁶¹ have found that the rate of nitronate addition depends on the basicity of the iminophosphorane used as the catalyst. However, with the more basic phosphazene catalyst studied here, there is spectroscopic evidence²² for the formation of a phosphonium-nitronate ion pair upon mixing of the neutral catalyst and nitromethane. Accordingly, we consider the deprotonation step relatively facile, and it has no influence over stereoselectivity since no stereocenters are formed in this step. Since formation of the reacting ion pair has been confirmed, we first tried to find the transition structures (TSs) corresponding to the stepwise addition of this complex to the aldehyde, followed by the protonation of the resulting alkoxide in a subsequent step. However, all our attempts to find any TS for the first step failed, even after including a tBuOH molecule (which may also be present in the reaction medium since the neutral catalyst is initially formed from the reaction of the catalyst:HCl salt with KOTBu) to stabilize the buildup of negative charge on the carbonyl oxygen through hydrogen bonding.

Considering that a plausible explanation for this failure is the unfavorable energetic cost of generating an alkoxide anion in the addition step, we thought that it could be possible to obtain these TSs by the inclusion of an additional molecule, which could transfer a hydrogen atom to the oxygen in the C–C bond forming step. We noticed that for the *in situ* preparation of the catalyst, a subequimolar amount of potassium tert-butoxide (typically 0.9 equiv) is employed. Therefore, there is a (small) amount of catalyst in its tetraaminophosphonium form that could potentially interact with the carbonyl. Within this hypothesis, C–C bond formation would require two catalyst molecules, one making an ion pair with the nitronate and a second to activate the carbonyl group. Proton-transfer from this second catalyst molecule to an aldehyde oxygen atom would avoid the formation of an unstable alkoxide intermediate, yielding a neutral, basic catalyst molecule that could react with nitromethane to reform the phosphonium:nitronate ion pair and continue the catalytic cycle (Scheme 2).

In its tetraaminophosphonium form, the organocatalyst contains four possible H-bond donors that are not equivalent: two NH groups are adjacent to a diphenyl-substituted carbon and two to an isopropyl substituted carbon. The bidentate H-bonding interaction of the catalyst with either the nitronate or the carbonyl involves two of these groups, and therefore, there are different combinations depending on which NH group is H-bonded to the substrate. The nitronate can make H bonds with the two NH adjacent to diphenyl-substituted carbon atoms (mode of activation “a” in Scheme 3), with the two NH adjacent to isopropyl-substituted carbon (“b” in Scheme 3), or with one of each. In this latter case, there are two different orientations (“c” and “d” modes of activation in Scheme 3, note that after including the benzaldehyde molecule these modes are not equivalent) of the catalyst. Accordingly, the aldehyde carbonyl can also establish two H bond with the catalyst in four different ways (denoted as “a”, “b”, “c”, and “d” in Scheme 3). Overall, there are 16 different combinations.

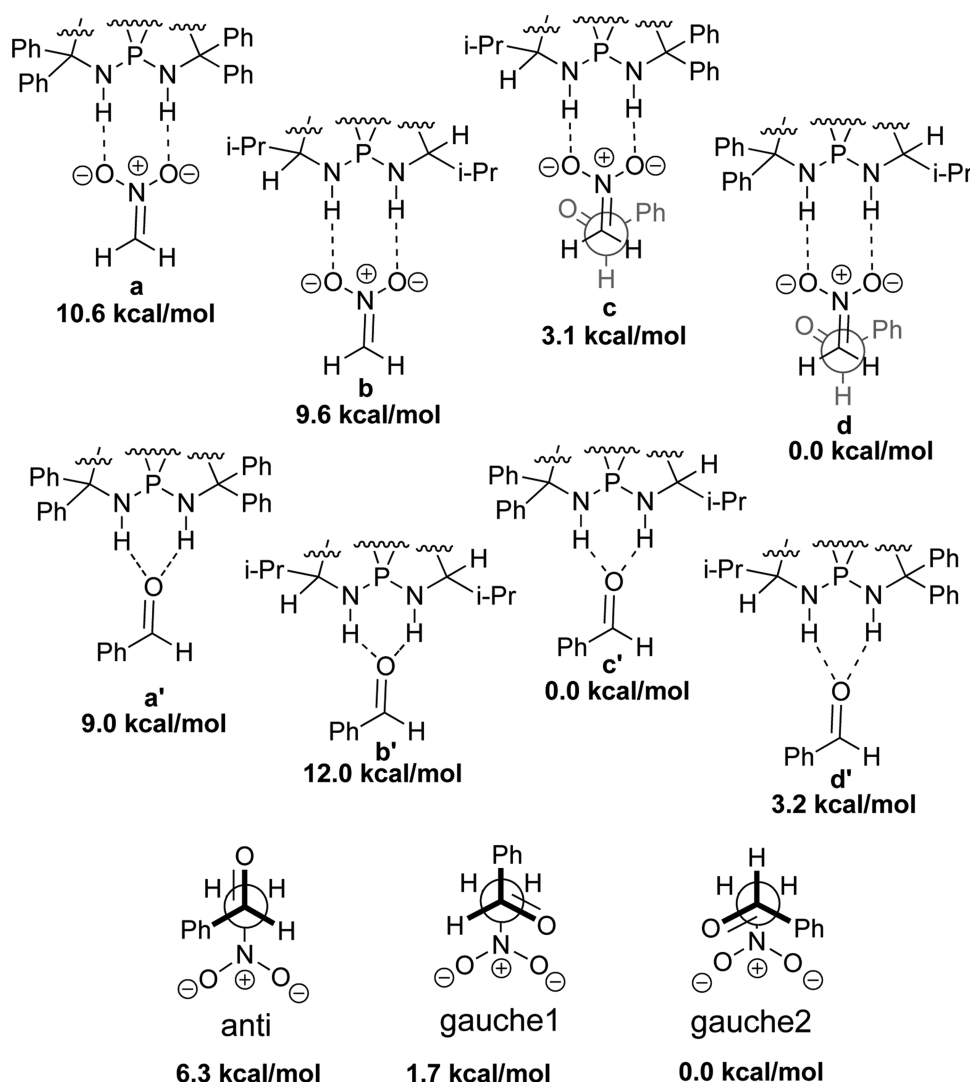
Scheme 2. Reaction Mechanism Involving Two Catalyst Molecules



Houk and Breugst⁶² have recently studied the mechanism of the Henry reaction catalyzed by chiral bistioureas. They contemplated three possible orientations of the nitromethane and the aldehyde: one anti and two gauche conformations. We also studied these three possibilities, and for consistency, we have adopted the same nomenclature as those authors (Scheme 3). Combined with the 16 different combinations of the catalyst orientation, we calculated 48 TS structures leading to the (*R*)-configured alcohol product and 48 leading to the (*S*)-product. In the interest of computational tractability, an explicit chloride counteranion is not included in these calculations, since its effects on the stereochemical outcome are expected to be negligible.

Full details of all structures and energies corresponding to this mechanism are included in the Supporting Information. Our nomenclature for computed structures refers to the mode of activation (*aa'*, *ab'*, etc.), the orientation of the reactants (*anti*, *gau1*, and *gau2* for *anti*, *gauche1*, and *gauche2*, respectively) and the absolute configuration (*R* or *S*) of the product obtained. We observed that all TS structures in which either the nitronate interacts with the catalyst by modes “a” or “b” or the carbonyl group by modes “a” or “b” are energetically infeasible, lying 9.0 kcal/mol or higher in free energy above the most stable structure, and therefore, this mode of interaction can be firmly rejected. This is consistent with the X-ray crystal structure of the chloride salt of catalyst 1a,²² in which the chloride anion establishes two hydrogen bonds with the catalyst by means of two nonequivalent NH groups (similar to modes “c” or “d” in Scheme 3).

Figure 1 shows the most stable TS structures, obtained for *anti*, *gauche1*, and *gauche2* orientations. The remaining, less stable, structures are shown in the Supporting Information. *Gauche2* TS structures are found to be more stable, in contrast with the results from Houk and Breugst⁶² for the uncatalyzed reaction between nitronate and benzaldehyde, where *anti* and *gauche1* orientation were more stable. This difference can be explained as the consequence of steric interactions between the catalysts and the

Scheme 3. All Possible Catalyst:Substrate Binding Modes and Conformations about the Forming C–C Bond Considered for TSs Involving Two Catalyst Equivalents^a

^aThe energy of the most stable TS structure corresponding to a conformation or mode of activation is also shown.

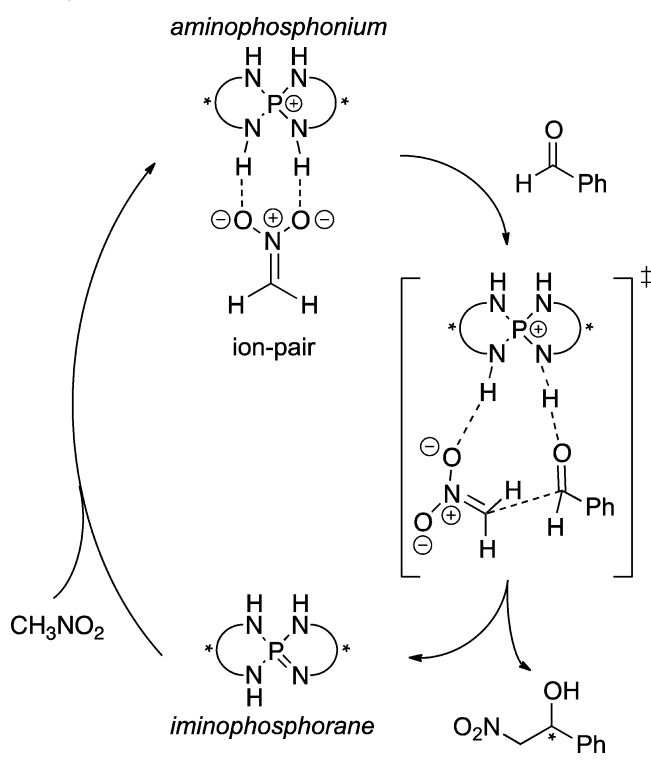
reactants, absent in the uncatalyzed reaction. In this mechanism, where two molecules of catalyst are required, computation predicts that the major enantiomer would have an (*R*)-absolute configuration. Experimentally, the (*S*)-configuration is the major enantiomer.²² On the basis of this discrepancy, and alongside the observation that the asymmetric reaction still occurs at catalyst loadings as low as 1 mol %, mechanisms invoking two molecules of catalyst participating in the selectivity determining step are unsubstantiated.

Henry Reaction: Single Molecule Catalyst Case. Since the mechanism involving two catalyst molecules is not able to account for the experimental results, we focused our attention on the action of a single catalyst molecule making an ion pair with the nitronate, which then also transfers a proton to the carbonyl group of the aldehyde. Two amino N–H groups of the catalyst play an active role in the mechanism: one making an H bond with the nitronate and a second with the carbonyl group (Scheme 4). Proton transfer to the developing alkoxide would then occur in a concerted manner along with C–C bond formation.

In this mechanism, there are four possible ways for the catalyst to interact with the TS: the nitronate and the carbonyl oxygen

can be H-bonded to an N–H bond adjacent to either a diphenyl-substituted or an isopropyl-substituted carbon. This gives rise to four possible modes of interaction between catalyst and TS, referred as “a”, “b”, “c”, and “d” in Scheme 5. Additionally, as in the previously proposed mechanism, it is necessary to consider three possible orientations of the nucleophile and the electrophile about the forming C–C bond (anti, gauche1, and gauche2). In gauche1 and gauche2 orientations, we found that the H-bonding interaction established between the nitronate and the catalyst was possible with either oxygen atoms of the nitro group. We term these possibilities as “syn” if the H-bonded nitronate oxygen and the aldehyde oxygen are on the same side and “anti” on the opposite side. Finally, the catalyst-nitronate H bond can show two different orientations with respect to the O=N bond (“Z-like” and “E-like” conformations). In the case of the anti orientation, the only possibility was that the nitronate oxygen directed away from the benzaldehyde phenyl group, since, otherwise, the catalyst would collide with it. Although we tried to locate TS structures for all these possibilities, in some cases during the optimization the geometry changed to yield a different orientation.

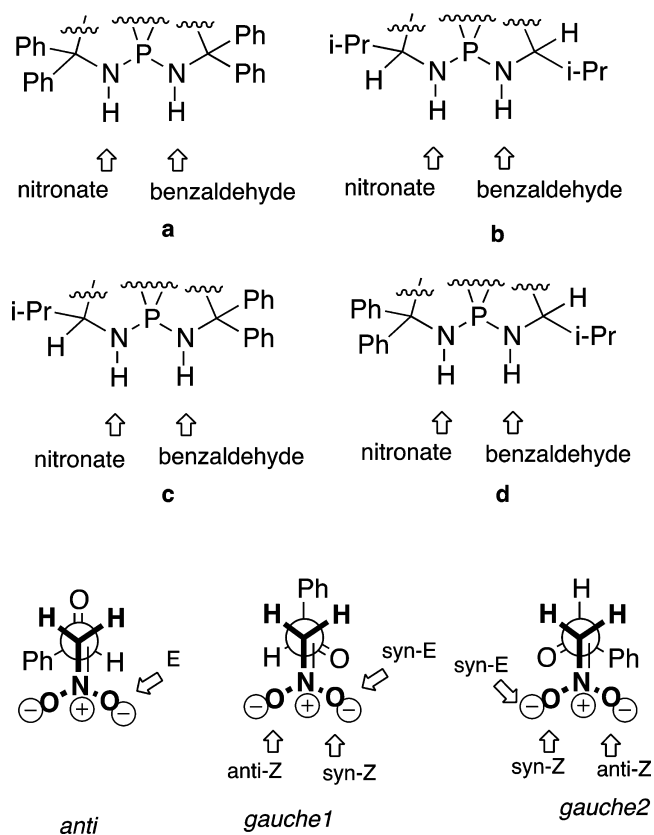
Scheme 4. Proposed Henry Reaction Mechanism with a Single Catalyst Molecule



We were able to optimize 27 TSs, leading to the (*R*)-adduct and 24 leading to the (*S*)-adduct, differing in terms of the H-bonding modes and conformations enumerated in Scheme 5. Structure names refer to the possible combinations of mode of activation, conformation, and orientation of the H bonds. Thankfully, many of these structures can be discounted: as we observed for structures involving two catalyst molecules, TS structures in which equivalent NH groups were involved (activation modes “a” and “b”) lie high in free energy (more than 3.2 kcal/mol above the most stable TS) and thus do not contribute significantly toward catalysis. This observation means that, while the structures of catalysts **1** and **2** are C_2 -symmetrical, catalytic activation itself involves the pairs of N–H protons that are unrelated through symmetry. Thus, nucleophilic and electrophilic reactants will experience a dissimilar steric and electronic environment from their interaction with the catalyst, in contrast to activation with, for example, chiral phosphoric acids. Furthermore, we have found that the preference of catalyst **1** to interact via nonequivalent N–H groups may be explained quantitatively in terms of the catalyst deformation/distortion energy. In order to accommodate the two reactants via modes a and b (Scheme 5), the catalyst must undergo greater geometric reorganization since the distance between symmetry-related protons is actually much greater in the catalyst’s optimal structure. There exists a positive, linear correlation between the computed TS energies and the energy required to distort/deform the catalyst in the TS (Figure S1 of the Supporting Information).

The preference for modes “d” and “c” means that, in contrast to many organocatalysts that interact by dual H-bonding interactions, chiral phosphacene **1** is not acting as a C_2 -symmetric catalyst. Catalyst **2**, also developed by Ooi and co-workers, only has two available amino groups for catalysis due to methylation of the two N atoms adjacent to isopropyl groups. The available N–

Scheme 5. All Possible Catalyst:Substrate Binding Modes and Conformations about the forming C–C Bond Considered for TSs Involving a Single Catalyst



H atoms are related by symmetry and therefore **2** is expected to function as a C_2 -symmetric catalyst, unlike **1**. This fact might contribute to explain differences in the behavior of both catalysts, such as the different protonation pathways observed in the Michael addition of azalactones to methyl-propiolate.³¹ Related to this, Terada and Takeda have recently described a chiral bis(guanidine)iminophosphorane catalyst.⁶³ While the X-ray crystal structure of the complex of the (*M*) diastereoisomer with HCl shows a C_2 symmetry axis, a similar complex of the (*P*) diastereoisomer lacks this symmetry. In this case, only the (*M*), C_2 symmetric catalyst shows enantioselectivity in the amination of cyclic ketones with di-*t*-butyl-aza dicarboxylate.

We also observed that TS structures that correspond to activation mode “d” were also high in energy (for the best “d” TS structure the energy was 3.6 kcal/mol higher than for the best “c” TS structure). In Figure 2, the *gau1* TS structures of this activation mode are shown. In *TS-d-gau1-Z-syn-R* and *TS-d-gau1-Z-syn-S*, to accommodate the nitronate close to the diphenyl group, the structure of the catalyst is strongly distorted, as revealed by the overlay of the catalyst in these TS structures compared with the X-ray crystallographic structure²² of the catalyst chlorohydrate salt. This shows the degree of “induced fit” distortion required by the catalyst to accommodate the two substrates. This distortion is not as severe in the case of *TS-d-gau1-Z-anti-R* and *TS-d-gau1-Z-anti-S*, probably because the nitro group is placed in a less hindered position, but the distance between the benzaldehyde oxygen and the nitronate oxygen involved in hydrogen bond formation is too large (3.5 and 3.7 Å) to fit well in the catalyst. A similar explanation justifies the high energy of *gau2* transition state structures.

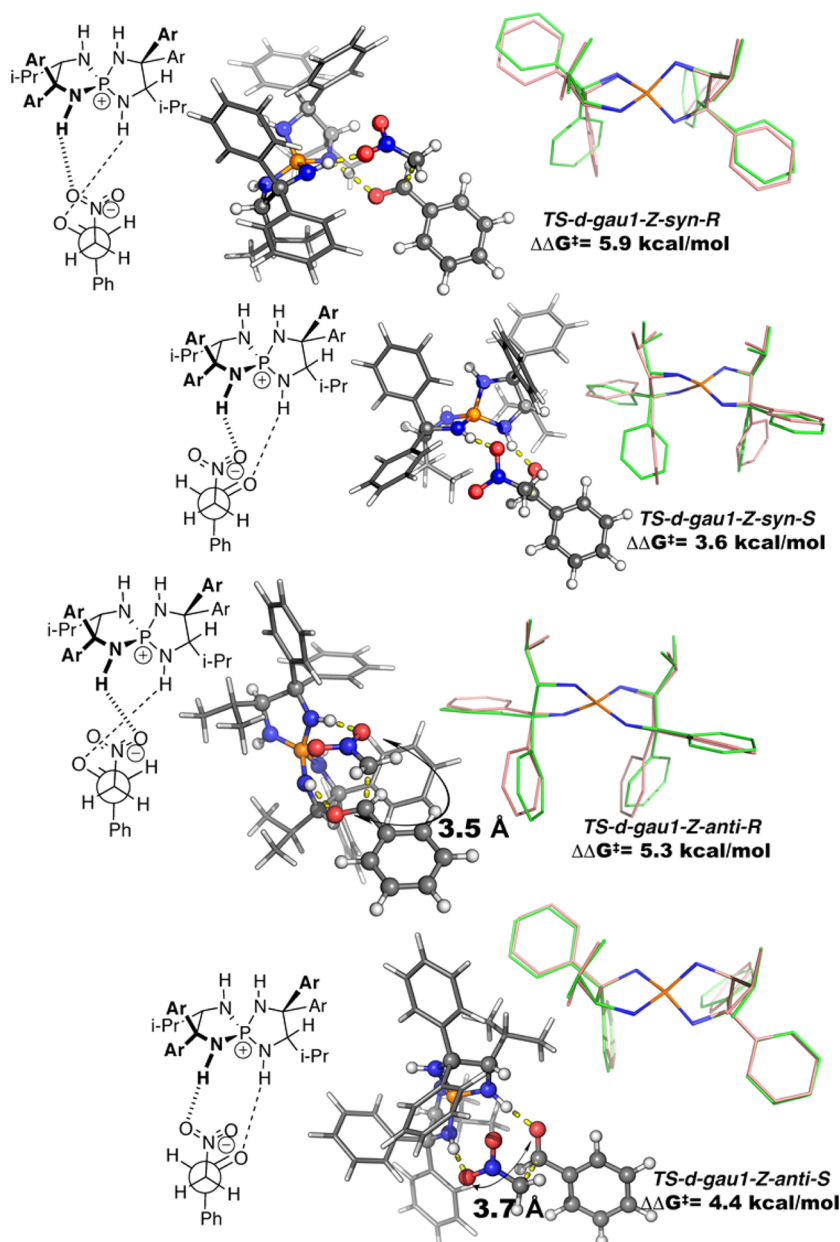


Figure 2. Most stable TS structures activation mode “d” with the gauche1 conformation. RHS shows overlay of the catalyst geometry in each TS with its X-ray structure.²²

The most stable TS structures were obtained for activation mode “c”. From the 3 orientations between the nitro and the carbonyl (Figure 3a), anti TS structures show very high energies. The distance between the two oxygen atoms is too large (3.9 Å in *TS-c-anti-R* and 3.5 Å, compared to the distance between the two nitrogen H-bond donors in the catalyst, 2.7 Å) to fit well in the catalyst. Indeed, in order to reduce this distance the two groups are almost eclipsed. The TS structures corresponding to gauche2 conformation also have higher energy than those corresponding to gauche1 conformation. In gauche1 TSs the benzaldehyde phenyl group is directed away from the catalyst, preventing steric interactions and contributing to more stable TS structures. In Figure 3b, structures of the most important gauche2 transition states are shown. In *TS-c-gau2-syn-Z-R*, to prevent the steric collision with the catalyst, the nitronate and benzaldehyde are almost eclipsed, with a dihedral angle of only 15°. In *TS-c-gau2-*

syn-Z-S it is the catalyst that is distorted, shown by the comparison of its geometry in this TS with the X-ray structure.

TS-c-gau1-Z-syn-R is destabilized by steric interactions between the nitronate oxygen not bonded to the catalyst and one of the isopropyl groups (Figure 4, above). In *TS-c-gau1-Z-anti-S*, in addition to this effect, the distance between the two O atoms is too long (3.4 Å).

The most stable, stereodetermining TS structures are *TS-c-gau1-Z-syn-S* and *TS-c-gau1-Z-anti-R* (Figure 4). The free-energy difference is 1.2 kcal/mol in favor of formation of the (*S*)-product. This is in excellent agreement with the experimental results (calculated: 90% e.e., Boltzman average including all calculated structures: 91.5% e.e.; experimental: 89% e.e.). In both TS structures, the nitronate oxygen atom that is not making a hydrogen bond with the catalyst is directed toward the hydrogen atom of the isopropyl-substituted carbon in the catalyst. An NCI calculation reveals the presence of a stabilizing interaction

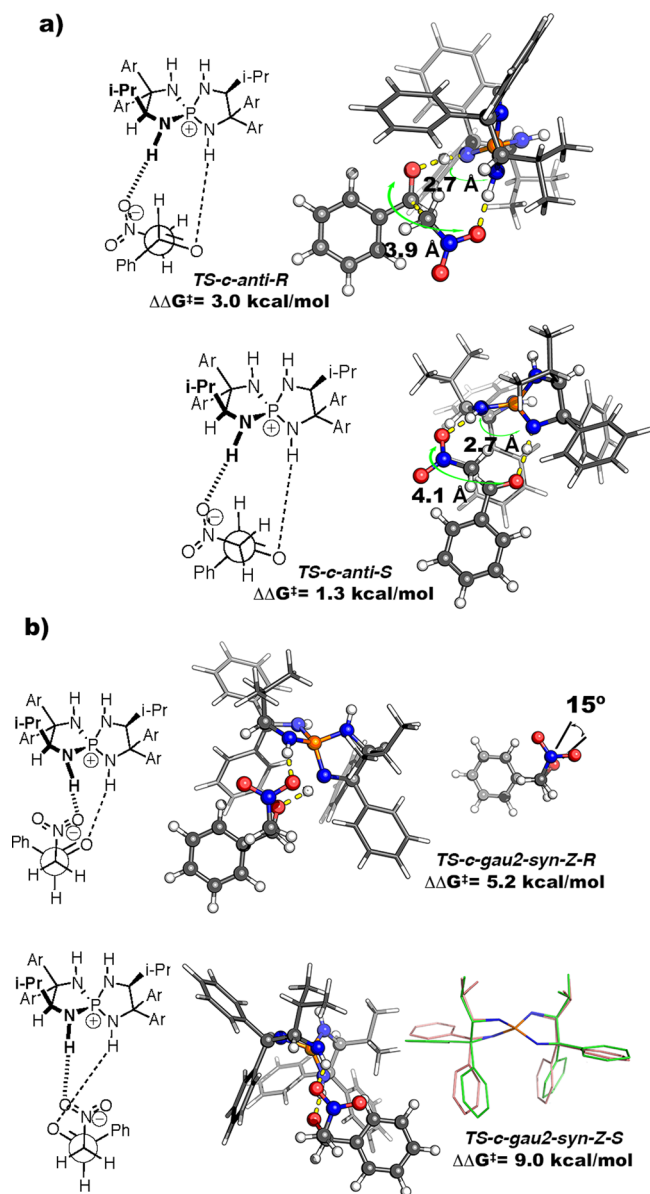


Figure 3. (a) The most relevant TS structures for mode of activation “c” and gauche1 conformation. (b) Representative TSs structures for mode of activation “c” and gauche2 conformation. RHS shows superimposition of the catalyst geometry in the TS with its X-ray structure.²²

between these two atoms. In addition, NCI analysis shows there are stabilizing interactions with the benzaldehyde oxygen and aromatic H atoms in the phenyl groups, and a C–H– π interaction between one aromatic ring and benzaldehyde hydrogen (shown by green isosurface in Figure 4). Therefore, this geometry prevents steric interactions between the catalyst bulky groups and the reactants. C–H \cdots O interactions have been found to play an important role in the stabilization of TS for different reactions,^{64–69} and they may also play an important role here. In the less stable *TS-c-gau1-Z-anti-R*, the dihedral angle around the forming C–C bond is only 30°; this distortion of the TS is needed to allow the formation of the hydrogen bond with the carbonyl oxygen and justifies the higher energy of this structure.

Henry Reaction of Nitroethane and Benzaldehyde Catalyzed by 1b Catalyst. We next studied the reaction of nitroethane with benzaldehyde catalyzed by **1b**. On the basis of

previous results, we only calculated structures corresponding to the “c” or “d” mode of activation, gauche1 orientation, and Z configuration of the nitronate H bond, although structures corresponding to mode of activation “d” show higher energies (4.0 kcal/mol in the best case).

As for the reaction of nitromethane, the most stable TS structures corresponds to a Z hydrogen bond configuration, with the nitronate oxygen on the same side as the carbonyl oxygen (*TS-c-gau1-Z-syn-SR* and *TS-c-gau1-Z-syn-SS*, Figure 5a). The energy difference between these structures is 1.2 kcal/mol (calculated anti/syn d.r.: 22:1), which is consistent with the experimental observed ratio of higher than 19:1. The most obvious difference between the two competing low-energy TS structures is the position of the nitronate methyl group: gauche conformation with respect to the benzaldehyde oxygen in the most stable TS and anti in the other. Considering that a gauche effect⁷⁰ may account for this energy difference, we evaluated the degree of hyperconjugation between the donor σ (C–H) orbital and acceptor σ^* (C–O) orbital using NBO calculations. While this stabilizing interaction is present in the (*R,S*)-diastereomer of the alcohol product (Figure 5b, 4.3 kcal/mol, c.f. 5.9 kcal/mol for a $\sigma_{C-H} \sigma^*_{C-F}$ interaction in 1,2 difluoroethane at an identical level of theory), it was not found in either TS (i.e., smaller than 0.5 kcal/mol in magnitude). A deeper exploration of these structures revealed that in the less stable *TS-c-gau1-Z-syn-SS* TS, the phenyl group in benzaldehyde rotates to prevent collision with the nitronate methyl group. A side effect of this rotation is that the dihedral angle with respect to the carbonyl bond is increased to 23°, reducing the conjugation between the carbonyl and phenyl groups (Figure 5c). In the *TS-c-gau1-Z-syn-SR* structure, this angle is 9°; although the difference is small, gas-phase single-point calculation on the benzaldehyde geometries extracted from *TS-c-gau1-Z-syn-SS* and *TS-c-gau1-Z-syn-SR* show a 0.9 kcal/mol more stable aldehyde in the SS-TS. This energy difference arises from the different dihedral angle, since the forming C–C bond distance is almost identical (2.09 Å) in each case.

Considering the attack of the opposite aldehyde enantioface, the most stable (*R*)-TS structures, *TS-c-gau1-Z-anti-RS* and *TS-c-gau1-Z-anti-RR*, are 2.0 and 3.3 kcal/mol higher in free energy, respectively. This computed free energy difference implies a 99% e.e. (of either diastereomer), very close to the 97% e.e. observed experimentally. The most stable TS leading to the major stereoisomer adopts the same conformation and binding mode as for the reaction with nitromethane.

Addition of Phosphonate to Benzaldehyde Catalyzed by 1a Catalyst. Finally, to test the generality of our proposed mechanism for the addition of nitronates to a different nucleophile, we calculated TS structures corresponding to the addition of dimethyl phosphonate to benzaldehyde catalyzed by **1a**.²⁴ As with the nitroaldol (Henry) addition, the most stable TS structures were obtained when the nucleophile makes a H bond with the NH group adjacent to the isopropyl-substituted carbon (binding mode c). Since the nucleophile is bigger and more demanding sterically, it occupies the less-hindered position in the catalyst. The benzaldehyde molecule preferentially orients the phenyl group away from the catalyst bulky groups, leading to a gauche1 conformation. In the most stable TS structure (*TS-gau1-R*), the C=O bond is directed toward the other NH bond donor in the catalyst (Figure 6). This TS structure yields the (*R*)-configured alcohol. However, note that the change in stereochemical assignment with respect to nitronate addition is due to a change in Cahn-Ingold-Prelog priorities: in all the reactions

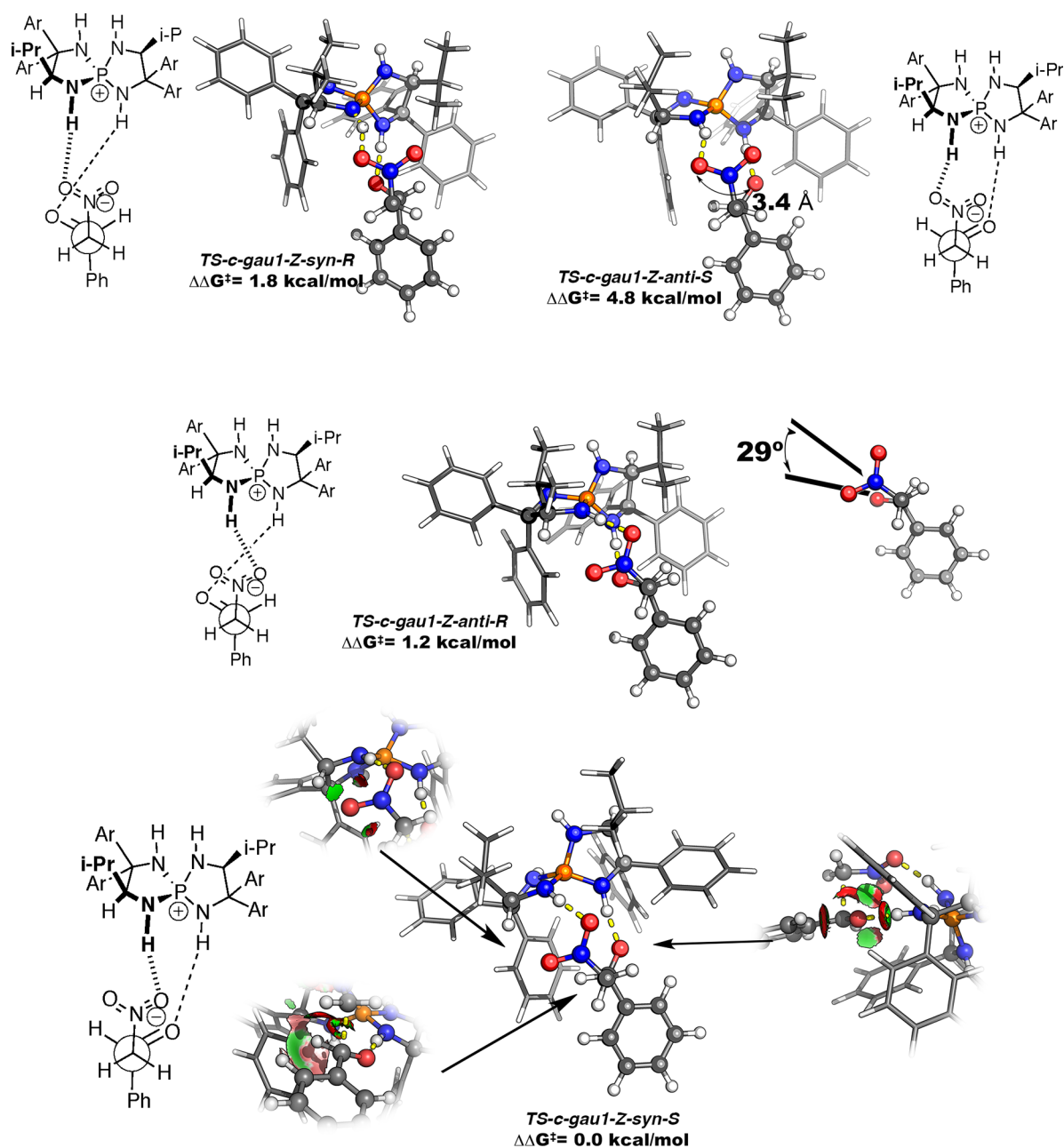


Figure 4. Most stable TS structures for the reaction between nitromethane and benzaldehyde catalyzed by **1a**. The NCI index in the lower TS is represented by the isosurface of electron density gradient colored by the second eigenvalue of the electron density Laplacian (green, negative eigenvalue, attractive interaction; red, positive eigenvalue, repulsive interaction).

studied, the electrophile adopts the same conformation and the reactants are bound similarly, such that the major enantiomer results from attack of the aldehyde Si face.

In order to obtain the (*S*)-enantiomer, it is necessary to deform the structure so the carbonyl group can make a H bond with the catalyst (*TS-gau1-S*) or to adopt a gauche2 conformation (*TS-gau2-S*). In this case, to prevent steric interactions with the catalyst, the phosphonate and the aldehyde are almost eclipsed. This TS lies 1.1 kcal/mol higher in free energy than *TS-gau1-R*. This implies that the (*R*)-product will be obtained in 88% e.e., in good quantitative agreement with the 85% e.e. obtained experimentally.²⁴ Interestingly, the absolute configuration of the major enantiomer has been assigned experimentally as (*S*) on the basis of elution times using chiral chromatography. Our computational result thus prompted further investigation, and

we observed that a different stationary phase had been used in the comparison experiments. We located literature data,⁷¹ published after Ooi's original work, that employs identical eluents and chiral stationary phase, and in which the same product is formed, where absolute configuration was assigned on the basis of optical rotation. On the basis of a comparison of these elution times [11.6 min for the (*R*)-enantiomer and 14.1 min for the (*S*)-enantiomer] with those published by Ooi (12.2 min for the major enantiomer and 16.0 min for the minor enantiomer), we believe that the major enantiomer obtained with catalyst **1a** should be revised to the (*R*)-configuration, which is fully consistent with our computational results (full details of the comparison of HPLC retention times are provided in the Supporting Information).

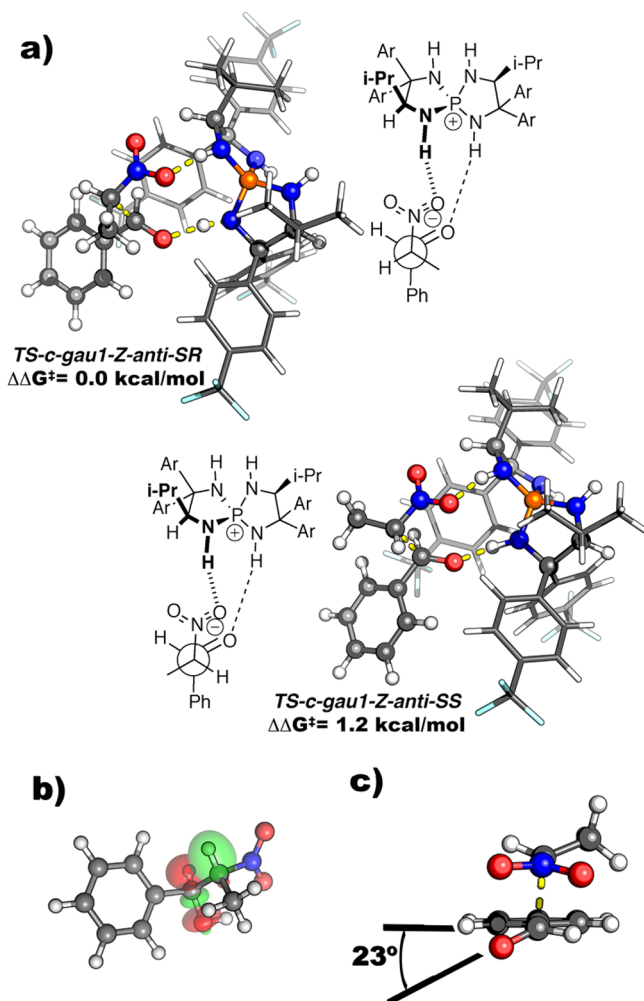


Figure 5. (a) TS structures for the reaction of nitroethane yielding (*R,S*) and (*S,R*)-2-nitro-1-phenyl-1-propanol. (b) Favorable hyperconjugation present in the product but not in the TS structures. (c) Dihedral angle between the phenyl and carbonyl groups in (*S,S*) TS.

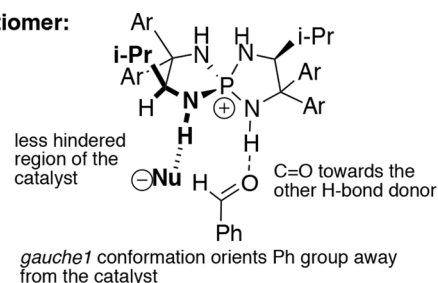
CONCLUSIONS

The mechanisms of both nitroaldol (Henry) and phosphite additions to aldehydes catalyzed by a chiral phosphacene catalyst have been investigated. After an extensive search of TS structures, we have been able to discount the mechanistic possibility of two catalyst molecules, one interacting with the nucleophile and another with the electrophile. Instead, experimental data agrees very well with our computed mechanism involving a single catalyst molecule that makes H bonds with the nucleophile and electrophile, transferring a proton to the electrophile preventing the negative charge accumulation on this atom. Mechanistically, the mode of action of this class of organocatalyst resembles the role established for other organocatalysts such as BINOP or guanidines. Importantly, however, unlike these catalysts, the catalytic mode of action of the tetraaminophosphonium does not preserve its C_2 symmetry, since two nonequivalent N–H groups are involved in substrate binding: the environments experienced by nucleophile and electrophile are thus inequivalent.

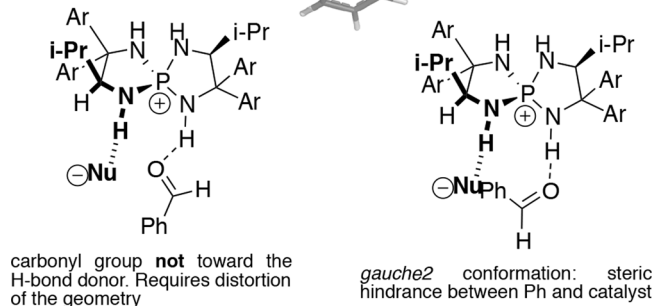
The most stable TS geometry for all of the reactions (nitro- and phospho-aldol reactions) considered here adopts the same substrate binding mode, in which the aldehyde adopts a common conformation leading to the attachment of the *Si*-enantiomeric

Scheme 6. Model for Predicting the Major Enantiomer of Reactions Catalyzed by Catalyst 1

major enantiomer:



minor enantiomer:



each case. In the case of dimethylphosphite addition, this has led us to revise the stereochemistry of the major enantiomer obtained experimentally, an assignment supported by comparison with experimental chiral chromatographic data. The most stable TS results from the formation of two anchoring H bonds with the reactants with minimal distortion of the catalyst structure and preserving the staggered conformation about the developing C–C bond. In less stable TSs, the catalyst must either undergo geometric distortion to form the H-bonding interactions, or unfavorable nonbonding interactions force the substrates to distort to staggered conformations.

From the calculations and their interpretation in terms of steric or CH–O interactions, it is possible to build a model to predict the stereochemical outcome of the reaction (Scheme 6). First, the catalyst uses two nonequivalent NH groups to interact with the substrates. The most sterically demanding substrate (in all these cases the nucleophile) makes an H bond with the NH group adjacent to the secondary carbon (the carbon substituted by the isopropyl group), since this is the less bulky position of the catalyst. In the case of nitronate addition, there is also a positive interaction between the C–H and one of the nitro oxygens. The aldehyde is bonded to the other NH group leading the phenyl group away from the catalyst (which means a preference for *gauche1* over *gauche2* conformations) since, otherwise, this group will collide with the catalyst bulky substituents. The most stable TS structure is obtained from the arrangement in which the carbonyl oxygen is directed toward the NH without needing a distortion of the structure.

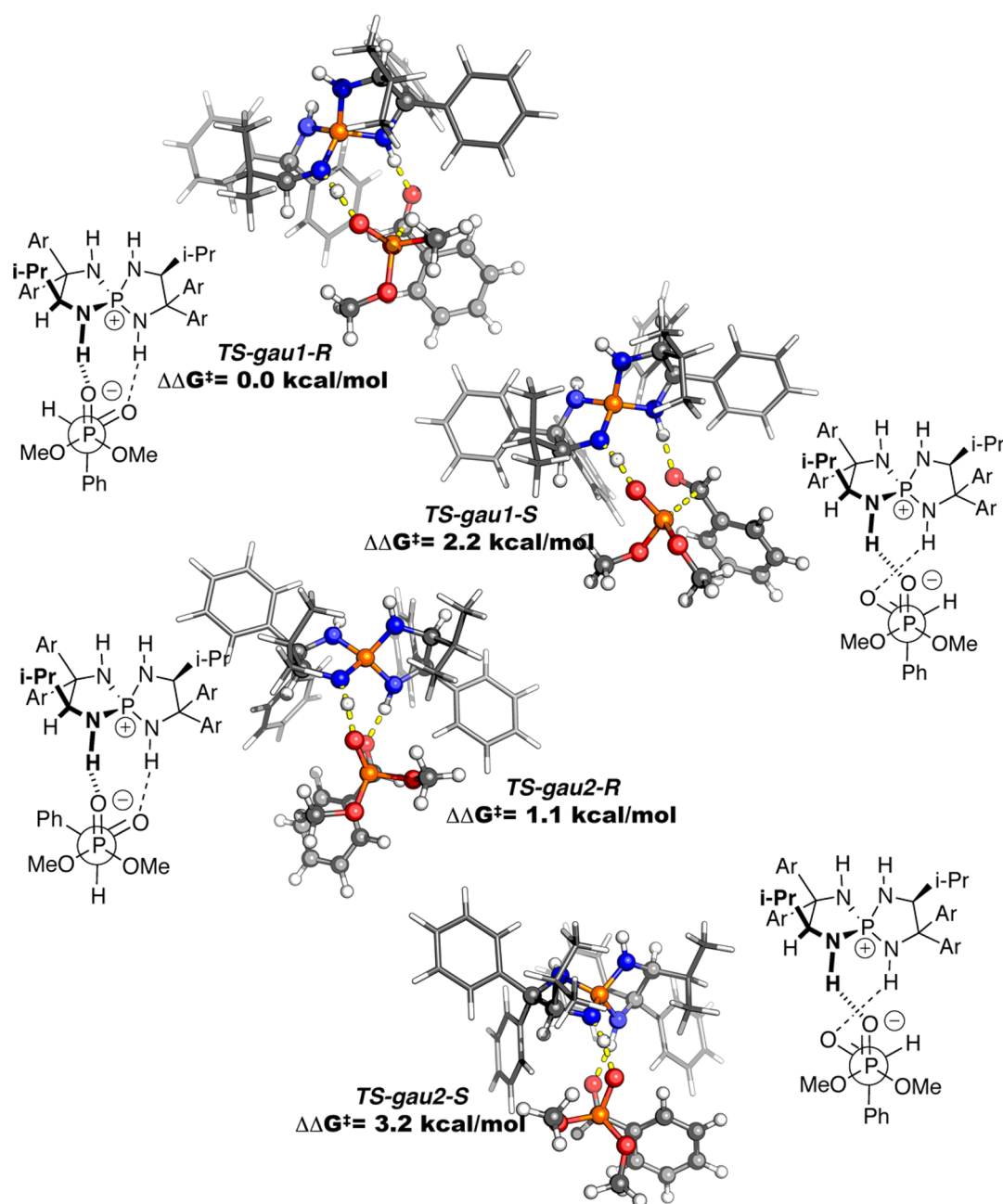


Figure 6. TS structures for the addition of dimethylphosphonate to benzaldehyde catalyzed by 1a.

■ ASSOCIATED CONTENT

📄 Supporting Information

Full ref 34. Correlation between catalyst distortion in the TS geometry and TS relative energy. All TS structures and their relative energies. Cartesian coordinates for all calculated structures. Assignment of the major enantiomer in the phosphoaldol reaction catalyzed by 1a. This material is available free of charge via the Internet at <http://pubs.acs.org>.

■ AUTHOR INFORMATION

Corresponding Authors

*E-mail: lsimon@usal.es.

*E-mail: robert.paton@chem.ox.ac.uk.

Notes

The authors declare no competing financial interest.

■ ACKNOWLEDGMENTS

We acknowledge the use of the EPSRC U.K. National Service for Computational Chemistry Software (NCS) at Imperial College London in carrying out this work.

■ DEDICATION

We would like to dedicate this work to the memory of Prof. Manuel Rico, pioneer in NMR spectroscopy, who recently passed away. Every single ppm of his wisdom was a source of inspiration.

■ REFERENCES

- (1) Simón, L.; Goodman, J. M. *J. Org. Chem.* **2007**, *72*, 9656.
- (2) Simón, L.; Goodman, J. M. *J. Am. Chem. Soc.* **2008**, *130*, 8741.
- (3) Simón, L.; Goodman, J. M. *J. Org. Chem.* **2011**, *76*, 1775.
- (4) Simón, L.; Goodman, J. M. *J. Am. Chem. Soc.* **2012**, *134*, 16869.

- (5) Marcelli, T.; Hammar, P.; Himo, F. *Chem.–Eur. J.* **2008**, *14*, 8562.
- (6) Marcelli, T.; Hammar, P.; Himo, F. *Adv. Synth. Catal.* **2009**, *351*, 525.
- (7) Li, J.; Jiang, W.-Y.; Han, K.-L.; He, G.-Z.; Li, C. *J. Org. Chem.* **2003**, *68*, 8786.
- (8) Susperregui, N.; Delcroix, D.; Martin-Vaca, B.; Bourissou, D.; Maron, L. *J. Org. Chem.* **2010**, *75*, 6581.
- (9) Jindal, G.; Sunoj, R. B. *Angew. Chem., Int. Ed.* **2014**, *53*, 4432.
- (10) Jindal, G.; Kisan, H. K.; Sunoj, R. B. *ACS Catal.* **2014**, 480.
- (11) Terada, M. *Chem. Commun.* **2008**, 4097.
- (12) Akiyama, T. *Chem. Rev. (Washington, DC, U.S.)* **2007**, *107*, 5744.
- (13) Leow, D.; Tan, C.-H. *Chem.–Asian J.* **2009**, *4*, 488.
- (14) Terada, M.; Nakano, M.; Ube, H. *J. Am. Chem. Soc.* **2006**, *128*, 16044.
- (15) Corey, E. J.; Grogan, M. J. *Org. Lett.* **1999**, *1*, 157.
- (16) Coric, I.; List, B. *Nature* **2012**, *483*, 315.
- (17) Chen, Y.-Y.; Jiang, Y.-J.; Fan, Y.-S.; Sha, D.; Wang, Q.; Zhang, G.; Zheng, L.; Zhang, S. *Tetrahedron: Asymmetry* **2012**, *23*, 904.
- (18) Rueping, M.; Nachtsheim, B. J.; Moreth, S. A.; Bolte, M. *Angew. Chem., Int. Ed.* **2008**, *47*, 593.
- (19) Vellalath, S.; Čorić, I.; List, B. *Angew. Chem., Int. Ed.* **2010**, *49*, 9749.
- (20) Werner, T. *Adv. Synth. Catal.* **2009**, *351*, 1469.
- (21) Enders, D.; Nguyen, T. V. *Org. Biomol. Chem.* **2012**, *10*, 5327.
- (22) Uraguchi, D.; Sakaki, S.; Ooi, T. *J. Am. Chem. Soc.* **2007**, *129*, 12392.
- (23) Uraguchi, D.; Ueki, Y.; Ooi, T. *J. Am. Chem. Soc.* **2008**, *130*, 14088.
- (24) Uraguchi, D.; Ito, T.; Ooi, T. *J. Am. Chem. Soc.* **2009**, *131*, 3836.
- (25) Uraguchi, D.; Ito, T.; Nakamura, S.; Ooi, T. *Chem. Sci.* **2010**, *1*, 488.
- (26) Uraguchi, D.; Nakamura, S.; Ooi, T. *Angew. Chem., Int. Ed.* **2010**, *49*, 7562.
- (27) Corbett, M. T.; Uraguchi, D.; Ooi, T.; Johnson, J. S. *Angew. Chem., Int. Ed.* **2012**, *51*, 4685.
- (28) Uraguchi, D.; Ueki, Y.; Ooi, T. *Chem. Sci.* **2012**, *3*, 842.
- (29) Uraguchi, D.; Yoshioka, K.; Ueki, Y.; Ooi, T. *J. Am. Chem. Soc.* **2013**, *135*, 8161.
- (30) Uraguchi, D.; Tsutsumi, R.; Ooi, T. *J. Am. Chem. Soc.* **2013**, *135*, 8161.
- (31) Uraguchi, D.; Ueki, Y.; Sugiyama, A.; Ooi, T. *Chem. Sci.* **2013**, *4*, 1308.
- (32) Uraguchi, D.; Nakamura, S.; Sasaki, H.; Konakade, Y.; Ooi, T. *Chem. Commun.* **2014**, *50*, 3491.
- (33) Uraguchi, D.; Tsutsumi, R.; Ooi, T. *Tetrahedron* **2014**, *70*, 1691.
- (34) Frisch, M. J.; et al. *Gaussian 09*, revision B.01, Gaussian, Inc.: Wallingford, CT, 2009.
- (35) Svensson, M.; Humbel, S.; Morokuma, K. *J. Chem. Phys.* **1996**, *105*, 3654.
- (36) Dapprich, S.; Komáromi, I.; Byun, K. S.; Morokuma, K.; Frisch, M. J. *J. Mol. Struct.* **1999**, *461*, 1.
- (37) Vreven, T.; Morokuma, K. *J. Comput. Chem.* **2000**, *21*, 1419.
- (38) Rappé, A. K.; Casewit, C. J.; Colwell, K. S.; Goddard, W. A., III; Skid, W. M. *J. Am. Chem. Soc.* **1992**, *114*, 10024.
- (39) Becke, A. D. *J. Chem. Phys.* **1983**, *98*, 5648.
- (40) Krishnan, R.; Binkley, J. S.; Seeger, R.; Pople, J. A. *J. Chem. Phys.* **1980**, *72*, 650.
- (41) Clark, T.; Chandrasekhar, J.; Schleyer, P. v. R. *J. Comput. Chem.* **1983**, *4*, 294.
- (42) Gill, P. M. W.; Johnson, B. G.; Pople, J. A.; Frisch, M. J. *Chem. Phys. Lett.* **1992**, *197*, 499.
- (43) Grayson, M. N.; Pellegrinet, S. C.; Goodman, J. M. *J. Am. Chem. Soc.* **2012**, *134*, 2716.
- (44) Simón, L.; Goodman, J. M. *J. Org. Chem.* **2010**, *75*, 589.
- (45) Simón, L.; Goodman, J. M. *J. Am. Chem. Soc.* **2009**, *131*, 4070.
- (46) Li, N.; Chen, X.-H.; Song, J.; Luo, S.-W.; Fan, W.; Gong, L.-Z. *J. Am. Chem. Soc.* **2009**, *131*, 15301.
- (47) *The PyMOL Molecular Graphics System*, version 0.99, Schrödinger, LLC: New York, 2010.
- (48) Chai, J.-D.; Head-Gordon, M. *Phys. Chem. Chem. Phys.* **2008**, *10*, 6615.
- (49) Cammi, R.; Mennucci, B.; Tomasi, J. *J. Phys. Chem. A* **1999**, *103*, 9100.
- (50) Cammi, R.; Mennucci, B.; Tomasi, J. *J. Phys. Chem. A* **2000**, *104*, 5631.
- (51) Cossi, M.; Rega, N.; Scalmani, M.; Barone, V. *J. Chem. Phys.* **2001**, *114*, 5691.
- (52) Cossi, M.; Scalmani, G.; Rega, N.; Barone, V. *J. Chem. Phys.* **2002**, *117*, 43.
- (53) Cossi, M.; Scalmani, G.; Rega, N.; Barone, V. *J. Comput. Chem.* **2003**, *24*, 669.
- (54) Marenich, A. V.; Cramer, C. J.; Truhlar, D. G. *Phys. Chem. B* **2009**, *113*, 6378.
- (55) <http://paton.chem.ox.ac.uk/software/software.html>.
- (56) Grimme, S. *Chem.–Eur. J.* **2012**, *18*, 9955.
- (57) Johnson, E. R.; Keinan, S.; Mori-Sánchez, P.; Contreras-García, J.; Cohen, A. J.; Yang, W. *J. Am. Chem. Soc.* **2010**, *132*, 6498.
- (58) Contreras-García, J.; Johnson, E. R.; Keinan, S.; Chaudret, R.; Piquemal, J.-P.; Beratan, D. N.; Yang, W. *J. Chem. Theory Comput.* **2011**, *7*, 625.
- (59) Glendening, E. D.; Weinhold, F. *J. Comput. Chem.* **1998**, *19*, 593.
- (60) Hammar, P.; Marcelli, T.; Hiemstra, H.; Himo, F. *Adv. Synth. Catal.* **2007**, *349*, 2537.
- (61) Nuñez, M. G.; Farley, A. J. M.; Dixon, D. J. *J. Am. Chem. Soc.* **2013**, *135*, 16348.
- (62) Breugst, M.; Houk, K. N. *J. Org. Chem.* **2014**, *79*, 6302.
- (63) Takeda, T.; Terada, M. *J. Am. Chem. Soc.* **2013**, *135*, 15306.
- (64) Corey, E. J.; Rohde, J. J.; Fischer, A.; Azimioara, M. D. *Tetrahedron Lett.* **1997**, *38*, 33.
- (65) Corey, E. J.; Lee, T. W. *Chem. Commun.* **2001**, 1321.
- (66) Paton, R. S.; Goodman, J. M. *Org. Lett.* **2006**, *8*, 4299.
- (67) Paton, R. S.; Goodman, J. M. *J. Org. Chem.* **2008**, *73*, 1253.
- (68) Johnston, R. C.; Cheong, P. H.-Y. *Org. Biomol. Chem.* **2013**, *11*, 5057.
- (69) Paton, R. S. *Org. Biomol. Chem.* **2014**, *12*, 1717.
- (70) Wolfe, S. *Acc. Chem. Res.* **1972**, *5*, 102.
- (71) Suyama, K.; Sakai, Y.; Matsumoto, K.; Saito, B.; Katsuki, T. *Angew. Chem., Int. Ed.* **2010**, *49*, 797.